Ampacity Calculation of the Underground Power Cables in Voluntary Conditions by Finite Element Method

S. Kahourzade[1], A. Mahmoudi[1,2], B. Nim Taj[1] and O. Palizban[1]
Babak.nimtaj@gmail.com, aminm@hict.edu.my, skahoorzade@yahoo.com, omid_pl@yahoo.com
[1] Electrical Engineering Department, University of Malaya, 50603 Kuala Lumpur, Malaysia.
[2] Engineering Department, Help College of Arts and Technology, Klang, 41050 Selangor, Malaysia.

***Abstract*- Exceeding the ampacity of the underground power cables according to the depth of soil and other parameters is a problem in literature because of the risk of temperature rise and subsequently the probable material failure. This paper introduces the heat transfer mechanisms in the underground cable installations and analyzes the available solution methods of the diffusion equation by finite element method. The cable ampacity is a function of soil thermal resistively, and burial depth. Cable ampacity relationship with these parameters is investigated and the manner that they affect the current of the cable is surveyed. To do so, the commercial ANSYS software has been employed. Results show that ampacity decreases as the depth of soil or its conduction thermal resistance increases. This method gives us the criteria and a flexible approach to change the strategy on those cases which have not been pointed in cable routing standard documentary.**

NOMENCLATURE

f	System frequency [Hz]
U	Cable operating voltage (phase-to-phase) [V]
θ	Conductor temperature [$^{\circ}C$]
T_{amb}	Ambient temperature [$^{\circ}C$]
H	Burial depth below the earth surface [m]
I	Current [Amp]
T	Operating temperature [$^{\circ}C$]
ρ	Thermal resistivity [$^{\circ}Km/w$]
S	Cross-sectional area of conductor [mm^2]
W_c	Losses in conductor per unit length [w/m]
W_I	Total RI^2 power loss of each cable [w/m]
W_d	Dielectric losses per unit length per phase [w/m]
W_t	Total power dissipated in the cable per unit [w/m]
ε	Relative permittivity of insulation
$tan\ \delta$	Loss factor of insulation
y_s	Skin effect factor
y_p	Proximity effect factor
D_i	Diameter over insulation [m]
d_c	External diameter of conductor [m]
λ_1	Ratio of the total losses in metallic sheath
λ_2	Ratio of the total losses in metallic armor
α_{20}	temperature coefficient at 20 degrees of Celsius
ρ_{20}	resistance at 20 degrees of Celsius
R'	dc conductor resistance [Ω/m]
R	ac conductor resistance [Ω/m]

I. INTRODUCTION

Calculation of the current-carrying capability or ampacity of power cables has been extensively discussed in the literature and is the subject of several international and national standards. Ampacity calculation techniques are as old as the cables themselves. Anders has summarized the history of ampacity calculations in his 1997 book [1]. There are analytical and numerical approaches to calculate cable ampacity. The two major international standard associations, the IEEE and the IEC, adopted the analytical methods as the basis for their standards [2], [3], [4]. The calculation procedures in both standards are the same in principle and are based on the model proposed by Neher and McGrath [5]. The major difference between them is the use of units and because of this, the same equations look completely different. The numerical approaches are mainly based on finite-difference or finite-element techniques. The finite-element technique is better suited for cable ampacity determination owing to physical condition of this problem.

Ampacity in an underground cable system is determined by the capacity of the installation to extract heat from the cable and dissipate it in the surrounding soil and atmosphere [6]. The maximum operating temperature of a cable is a function of the damage that the insulation can suffer as a consequence of high operating temperatures. The insulation withstands different temperatures as function of the duration of the current circulating in the conductors. There are three standardized ampacity ratings: steady state, transient (or emergency) and short-circuit. Only steady state ampacity ratings are discussed in this paper. As providing analytical solution for complex situation is very indirect, in many cases the experimental method may preferred. In these condition numerical methods such as finite element method (FEM) is more pragmatic and cost effective. This paper focuses on the numerical techniques for the computation of cable ampacity in steady-state through the use of assumptions that simplify the problem.

FEM is chosen to calculate the heat transfer field and heat

generation with in the cable and heat dissipation in the surrounding soil. ANSYS software is used to generate and solve the problem [7]. A two dimensional model of the cable in full size and surrounding area are designed in ANSYS. Results are then compared to values presented in standard tables. Also the skin effect in the isolation is considered as a reduction in the main current. Both three-phase and single-phase cable systems installed in standard condition is simulated and the temperature contour of them is presented. To investigate the effects of cable depth and soil thermal resistivity; these parameters are changed step by step and the ampacity of the cables in each case is calculated.

II. MODELING

The cable laying example shown in Fig. 1 is used to develop the mathematical model. It is a *400kV*, paper-polypropylene-paper cable with *2000mm²* copper segmental conductor and aluminum corrugated sheath. The outer covering is a PE jacket. The cable cross section is shown in Fig 2. The cables are laid in a flat formation without transposition, directly in the soil, with thermal resistivity of *1 °K.m/w* and ambient temperature equal to *25° C*. The sheaths are cross bounded with unknown minor section length. The centers of the cables are *1.8m* below the ground and phases are *0.5m* apart. This laying condition is called the standard installation. The cable parameters are provided in table I.

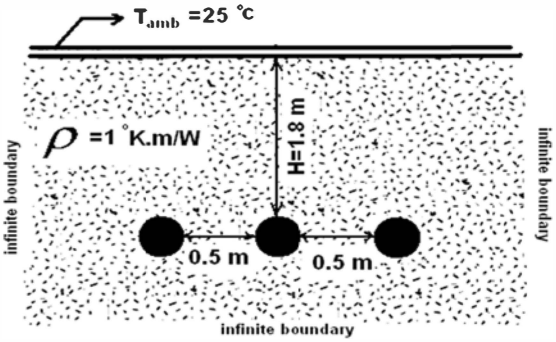

Fig. 1. Standard installation of the cable system

To consider the effect of infinite area around the cable and heat dissipation in this area to be reasonable minimum 100 meter of soil in every direction is considered, and isothermal boundary condition is then loaded as far beyond condition. As the soil conductivity is a great amount compare to the convection resistance of the air on earth surface, convection resistance of the air is neglected and the soil surface is considered as an isothermal surface. ANSYS analysis relies on its element and choosing the element has an important effect on the results. PLANE35 (a 6-node triangular element) is selected for simulations. The triangular shape element is well suited to model irregular meshes. The element has one degree of freedom, temperature at each node. The 6-node thermal element is applicable to a 2-D, steady-state or transient thermal analysis.

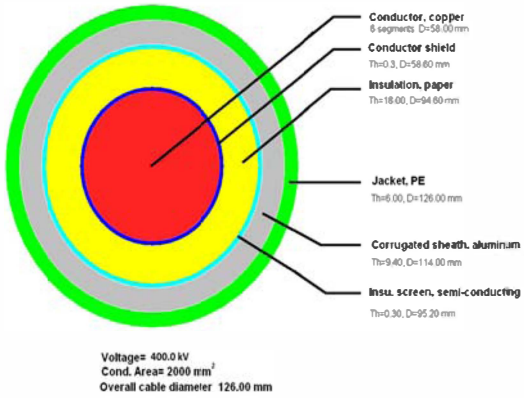

Fig. 2. Cable cross section

TABLE I
SOME PARAMETERS OF THE SIMULATED CABLE

General Data			
θ	85°C	ε	2.8
f	60 (*Hz*)	$tan\delta$	0.001
D_i		d_c	0.058
Calculated data for 3-phase cable system in standard installation			
y_s	0.132	y_p	0.005
λ_1	0.150	λ_2	0
R	0.0126 (Ω/km)	W_C	23.40 (*w/m*)
WI	26.92(*w/m*)	W_d	6.53 (*w/m*)
I	1365 (*Amp*)	W_T	33.45 (*w/m*)

Boundary conditions are isothermal (25 degrees of Centigrade) and heat generation in the cable conductor enters as a load. An iterative method is used to calculate ampacity of the cable. Also, the skin effect in the isolation is considered as reduction in the main current. Maximum temperature of power cables is determined by the cable insulation. This temperature is produced by the energy which is generated through Ohmic losses. dc conductor resistance R' *(Ω/m)* is first obtained from the following equation:

$$R' = \frac{1.02 \times 10^6 \rho_{20}}{S}[1 + \alpha_{20}(\theta - 20)] \quad (1)$$

R' is then modified to take into account skin and proximity effects. The resistance of a conductor when carrying alternating current is higher than that when carrying direct current. The principal reasons for the increase are skin effect, proximity effect, hysteresis and eddy current losses in nearby ferromagnetic materials, and induced losses in short-circuited non-ferromagnetic materials. For conductor losses, only skin and proximity effects, and in some cases approximation of metallic sheath effect, are considered, except in very high voltage cables consisting of large segmental conductors. The relevant expressions are:

$$R = R'(1 + y_s + y_p) \quad (2)$$

$$W_c = R \cdot I^2 \quad (3)$$

where, *R(Ω/m)* and W_c*(w/m)* are the conductor's ac resistance and losses, respectively. Sheath losses are current and bonding dependent, and can be divided into two categories. The losses are due to current circulating in single-

core-cable and divided in to eddy current circulating radially (skin effect) and azimuthally (proximity effect). Regardless of bonding, eddy current losses occur in both three-core and single-core cables. Eddy current losses in solidly bonded single-core-cable sheaths are negligible. So, they are ignored except for cables with large segmental conductors. Cable losses W_I can thus be expressed as:

$$W_I = W_c + W_s + W_a = W_c(1 + \lambda_1 + \lambda_2) \quad (4)$$

λ_1 is called sheath loss factor, and is equal to the ratio of total losses in the metallic sheath to total losses. λ_2 is armor loss factor, and is equal to the ratio of total losses in the metallic armor to total losses of conductor. When paper and solid dielectric insulations are subjected to alternating voltage, they act as large capacitors. Each time voltage direction changes, realignment of electrons produce heat. It results in loss of real power called dielectric loss. For a unit length of cable, magnitude of the required charging current is a function of dielectric insulation constant, dimensions of the cable, and operating voltage. For some cable arrangements (notably for high-voltage, paper insulated) this loss can significantly affect cable rating. Dielectric losses are computed from the following expression:

$$W_d = 2\pi \cdot f \cdot C \cdot U_0^2 \cdot \tan\delta \quad (5)$$

Where, the electrical capacitance C and the phase to ground voltage U_0 are obtained from:

$$C = \frac{\varepsilon}{18 \ln\left(\frac{D_i}{d_c}\right)} \cdot 10^{-9} \quad (6)$$

$$U_0 = \frac{U}{\sqrt{3}} \quad (7)$$

It is convenient to express all heat flows due to power losses in the cable in term of the loss per meter of the conductor. From Eqs. (4) and (5) the total loss W_t is computed from:

$$W_t = W_I + W_d = W_c(1 + \lambda_1 + \lambda_2) + W_d \quad (8)$$

Finally, heat generation applied to the conductor surface in the simulations is obtained from [8]:

$$H \cdot G = \frac{W_t}{S} \quad (9)$$

III. Simulation

A three-phase cable in standard installation is simulated by the ANSYS software and then a single-phase cable that is installed in its standard condition is simulated. Simulation method in both three-phases and single-phase is the same; the only difference is number of the cables. The temperature contour is presented for both three-phase and single-phase cable installation in Figs. 3 and 4 respectively.

In three-phase cable achieving 85°C restricts the current by 1363 *Amp*. In single-phase cable installation, the accepted current is limited by 1739 *Amp*. Current of three-phase and single-phase cable systems in standard installation are 1365 *Amp* and 1735 *Amp* respectively. The standard values indicate less than 1 percent difference compare to the results of simulation. Table II compares the simulated results with standard values. The results are very close to the ones presented in the standard that shows the validity of present simulation approach. Also, simulation results show that there is a significant cable ampacity reduction when the cable is used in three-phase installation (around 28 percent).

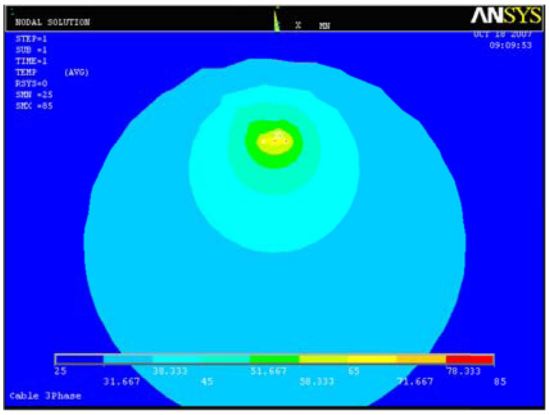

Fig. 3. Temperatures counter of the three-phase cable installation

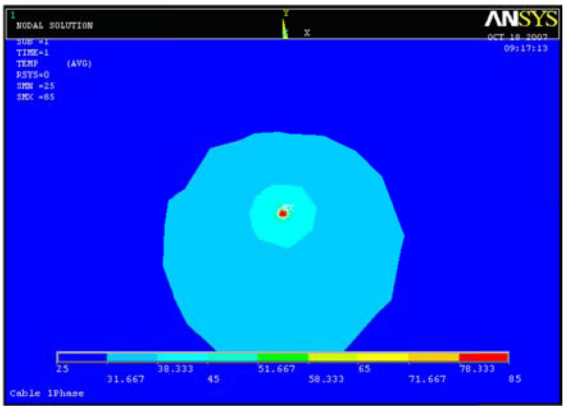

Fig. 4. Temperatures counter of the single-phase cable installation

TABLE II
SIMULATION AND STANDARD VALUES

	ANSYS Simulation	*Standard*	*Deviation from standard*
Three-phase	1363	1365	0.00146734
Single-phase	1739	1735	-0.00230017

IV. Analyses of Results and Parameter Effect

Effect of burial depth is shown in Figs. 5 and 6 for three-phase and single-phase cable installation, respectively. they show that with any increase in depth of the soil, its conductivity is reduced, less heat dissipation occurs and ampacity drops. The rate of cable ampacity variation is much more intense when the cable is buried near the earth surface than it is buried in depth.

Soil conductivity varies in soils with different properties

and its variation depends on moisture and substance content of the soil. Figs. 7 and 8 show the amount of cable ampacity against the soil resistivity variation for both three-phase and single-phase cable installation respectively. Cable ampacity is proportionate to soil conductivity; as soil conductivity raise, cable ampacity increases because more heat dissipation occurs.

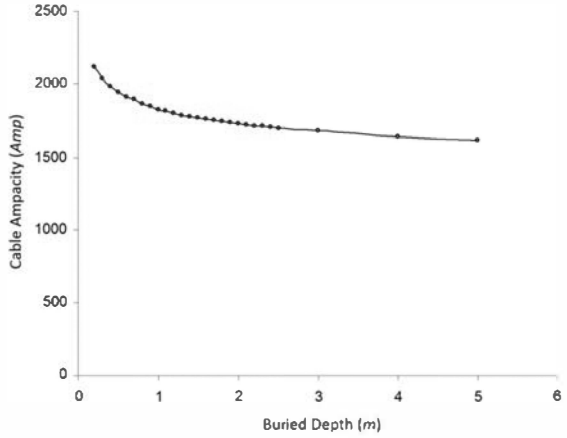

Fig. 5. Effect of buried depth variation of cable ampacity (Three-phases cable installation)

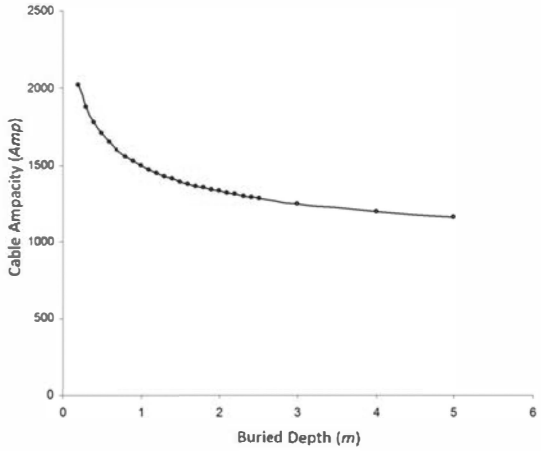

Fig. 6. Effect of buried depth variation on cable ampacity (single-phase cable installation)

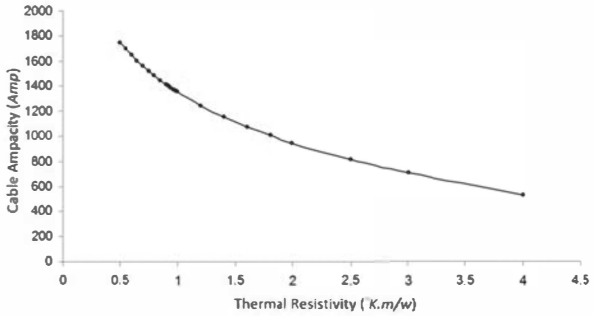

Fig. 7. Effect of soil thermal resistivity variation on cable ampacity

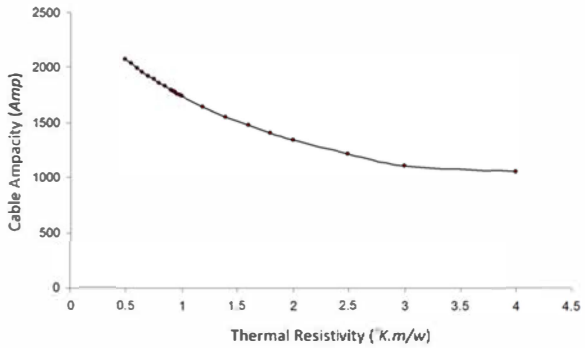

Fig. 8. Effect of soil thermal resistivity variation on cable ampacity (Single-phase cable)

V. Conclusion

To determine more closely the relevant temperature rises including the effects of soil conductivity and buried depth of cable is possible by the use of finite element method. The proposed model was used to determine fairly well the maximum allowable load currents for the cable under consideration. Such a model and analysis can be applied for assessing the ampacity of cables in various installation conditions. Results showed the amount of cable ampacity depends on the cable geometry, cable construction, burial depth and thermal conditions of the soil. Cable ampacity decreased as the depth of soil or its conduction thermal resistance increased. Also, cable ampacity reduces considerably when the cable is used in three-phase installation compared to single-phase installation. This method gives us the criteria and a flexible approach to change the strategy on those cases which have not been pointed in cable routing standard documentary.

VI. References

G.J. Anders(1997), "Rating of Electric Power Cables-Ampacity Calculations for Transmission, Distribution and Industrial application," IEEE Press, New York, McGraw-Hill(1998).

IEEE Standard Power Cable Ampacity Tables, 1994. IEEE Std. 835-1994, NY.

IEC Standard 60287 (1969, 1982, 1994), "Calculation of the continues current rating of cables (100% load factor)" 1st edition 1969, 2nd edition 1982, 3rd edition 1994-1995.

IEC Standard 60287, part 2-1 (1994), "Calculation of thermal resistances."

J. H. Neher and M. H. McGrath, "The calculation of the temperature riseand load capability of cable systems," AIEE Trans. Power App. Syst, vol.76, pp. 752–772, Oct. 1957.

G.J. Anders, "Rating of Electric Power Cables in Unfavorable Thermal Environments" IEEE Press, New York, (2005).

ANSYS Finite Element Simulation Software, ANSYS Inc., Canonsburg, PA.

A. Mahmoudi, "Ampacity Derating Factors for Cables in Different Environmental Conditions by FEM," M.S. dissertation. Dept. Elect. Eng., Amirkabir University of Technology, 2008.